

Anomalous hydrogen diffusion in VCr alloys: Trapping hydrogen via shallow potential well domains

Shu-Ming Wu^a, Chang-Chun He^a, Yu-Jun Zhao^a, Rong Liu^{b,*}, Xiao-Bao Yang^{a,*}

^a Department of Physics, South China University of Technology, Guangzhou, 510000, China

^b School of Electric Power, South China University of Technology, Guangzhou, 510000, China

ARTICLE INFO

Article history:

Received 15 November 2022

Received in revised form 25 January 2023

Accepted 10 February 2023

Available online 24 February 2023

Communicated by L. Ghivelder

Keywords:

VCr binary alloy

Hydrogen diffusivity

Kinetic Monte Carlo

ABSTRACT

In this paper, the dynamic of hydrogen diffusion in the VCr alloy is investigated by the first-principles calculations and kinetic Monte Carlo method. First, the structural stability as a function of components is explored, where the stable configurations hold high symmetry. For the stable structures, the hydrogen diffusivity is found to decrease first and then increase as the Cr content increases. The hydrogen diffusivity is calculated to be the slowest in $V_{0.375}Cr_{0.625}$, a structure with the space group $P4/mmm$. The results show that the main factor affecting the diffusion is not only the magnitude of a single barrier, but the overall spatial distribution of barriers, correspondent to the distribution of Cr atoms in VCr alloy. Furthermore, an unbalanced one-dimensional random walk model is proposed to well describe the phenomenon of anomalous hydrogen diffusion and elucidate the mechanism of hydrogen migration in the alloy.

© 2023 Published by Elsevier B.V.

1. Introduction

Hydrogen atoms can easily enter metallic alloy and cause unexpected catastrophic failures of materials, because they are the smallest and most abundant element in the earth. The penetration of hydrogen has a deleterious impact on the mechanical performance of alloy, which is known as hydrogen embrittlement [1–3]. Hydrogen embrittlement involves the accumulation of hydrogen at small microstructure flaws, leading to metal embrittlement and deterioration, which is a significant factor for the service life of metallic alloy [4–6]. Because the direct measurement of hydrogen diffusion is difficult to perform in experiment, theoretically determining the hydrogen diffusion coefficient of a given alloy is critical to enhance the hydrogen storage ability. Furthermore, investigating the hydrogen adsorption and desorption on the metallic alloy surfaces, hydrogen diffusion and trapping of the metallic alloy need to be fully explored. The hydrogen adsorption and desorption can only infer the static consequence with the absence of dynamic information. Therefore, probing the dynamic process of hydrogen atoms in metallic alloy can uncover the mechanism of hydrogen behavior of metallic alloy.

Theoretically, the diffusion is thought to be primarily determined by the prefactor (D_0) and the activation energy barrier [7,8]. A high barrier can effectively restrict hydrogen migration, reducing the diffusivity by trapping hydrogen in a specific area. Jiang and Carter et al. found that the hydrogen hopping barrier in the sub-surfaces of Fe(110) is higher than that in the pure bcc iron bulk, lowering the diffusivity coefficient [9]. J. Sanchez et al. calculated the barrier by the linear simultaneous transition method, and discovered that an external stress of several GPa resulted in a 10% change in the barrier and a 30% increase in the diffusion rate. At the same time, the structure has an impact on the diffusion bcc decreases the hopping barrier from 127 meV to 82 meV, resulting in faster diffusion [10]. Solid solution alloys of body centered cubic (BCC) structure are the promising future hydrogen storage materials. However, hydrogen diffusion is found to be not simply restricted by deep traps. Semidey-Flecha et al. reported that the presence of Ag in $Pd_{96}Ag_4$ decreased the hopping barrier between adjacent sites, but the sites close to the Ag atoms still effectively acted as traps for restraining hydrogen, decreasing the net diffusion of hydrogen, resulting in a slower net hydrogen diffusion than pure Pd [11]. It is shown that the diffusion does not completely depend on the hopping barrier, but also has an important relationship with the distribution of the hopping barrier. The VCr binary alloy is the BCC isomorphous [12], in which V and Cr can randomly dissolve in another. Because Cr is the neighbor of V, Cr is often used to synthesize V based hydrogen storage alloys, for example,

* Corresponding author.

E-mail addresses: liurongwrm@scut.edu.cn (R. Liu), scxbyang@scut.edu.cn (X.-B. Yang).

VTiCr alloys of a BCC structure [13,14]. The hydrogen diffusion has been investigated experimentally only in the VCrH phase through electric resistivity [15] and gas absorption methods. However, to our knowledge, the effect of Cr content of VCr alloy on hydrogen storage has not been extensively explored both in experiment and theory.

Previous experimental studies have reported that doping pure V with Cr (5% - 10%) will slow down diffusion [16,17] and restrict hydrogen diffusion, hence preventing hydrogen embrittlement [18]. It is impossible to determine all potential barriers exactly due to the diversity of alloy structures as a function of concentration. For the FeCr alloy, Samin et al. have estimated the potential barrier using the model and the associated potential barrier is smaller than that in the pure phase, while the calculated diffusion coefficient of hydrogen in the alloy is several orders of magnitude lower than that in the pure phase [19]. They speculated that hydrogen would sink in the region of the FeCr alloy where Cr accumulates. Hydrogen would similarly diffuse quickly once escaping the trap, but it would simply sink in another domain with Cr accumulation again.

Focusing on the VCr alloy, we have systematically investigated the evolution of the stable structure of the alloy with the composition by the first-principles calculations, simulating the diffusion process of hydrogen in the alloy with high symmetry distribution. The results reveal that the net diffusion rate is determined by the spatial distribution of the barrier, rather than its height. The alloy contains a series of continuous closed reversible potential wells that trap hydrogen atoms in the potential well domain, which will significantly slow down the hydrogen diffusion in the alloy. We have also proposed an effective model to explain the anomalous diffusion.

2. Calculation details

2.1. First-principles calculation

The first-principles calculations have been performed using the Vienna Ab-initio Simulation Package (VASP) [20,21], with the version of vasp 6.1.2. The generalized gradient approximation (GGA) [22,23] with the projector augmented wave (PAW) pseudopotentials in the Perdew-Burke-Ernzerhof (PBE) correlation was used to describe the Coulomb interactions between ion nuclei and valence electrons. The $5 \times 5 \times 5$ k -mesh in the irreducible Brillouin zone and the cut-off energy as 350 eV were adopted after a convergence test respectively. The spin polarized calculation was considered for all alloy structures, where the relaxation was fully conducted until the total forces on each atom were smaller than 0.01 eV/Å. Climbing-image nudged elastic band (CI-NEB) calculations [24] containing at least five images along the reaction coordinates, were also performed to identify the transition state for H migration between sites, and adopted to determine the transition states (TS). The convergence criterion is set to 0.03 eV/Å.

For the $V_{1-x}Cr_x$ alloy system, the mutual substitution components are in a same lattice structure to ensure a higher solid solubility during practical fusion process. The $2 \times 2 \times 2$ body-centered lattice supercell was used to generate a vanadium-based alloy. To investigate the formation enthalpy of VCr alloys at different concentrations in supercells, we searched out all possible structures for comparison. Removing the equivalent structures by the structural recognition and searching for unequal hydrogen interstitial sites in certain structures is employed by the SAGAR software [25].

2.2. Kinetic Monte Carlo simulation of hydrogen diffusion

We use the tetrahedral subdivision approach to find the interstitial position for the hydrogen diffusion, identifying the un-

equal positions for H atoms and determining the unequal transition paths. The diffusion barriers of all the possible transition paths are obtained by the NEB method. The hydrogen concentration in diffusion simulation is relatively low and the influence of hydrogen atom is very weak, so the hydrogen atoms in VCr structure have little influence on the calculated to energy landscape. As a result, we can observe the potential well domain from the potential energy surface. This work employs the Kinetic Monte Carlo (kMC) method to investigate the hydrogen atom diffusion path in the alloy and determine the diffusion coefficient. The harmonic transition state theory [26] gives the hopping rate R_q of the hop process q . $R_q = \nu e^{-E_{\text{barrier},q}/(k_B T)}$, where ν is the prefactor, which should be approximately 10^{13} /s [27,28], $E_{\text{barrier},q}$ is the process q energy barrier, k_B is the Boltzmann constant, and T is the absolute temperature. In the simulation, the temperature range is from 300 K to 1000 K.

The schematic flow chart of kMC method is shown in the supplementary materials. At each kMC step, we count all current possible processes R_{tot} and allocate processes based on the rate using random numbers, where $\Delta t = -\ln(\alpha)/R_{tot}$ is the simulation time of a single step hop (α is a random number within (0, 1)). The diffusion coefficient is calculated in our simulation by running at least 10^6 steps and eliminating the first 10^4 steps (to eliminate any transient behavior). The mean-squared displacement of each simulation is recorded by using [19,29,30]:

$$D = \lim_{t \rightarrow \infty} \frac{1}{2dtN_H} \sum_{i=1}^{N_H} |r_i(t) - r_i(0)|^2, \quad (1)$$

where t is the time, d is the simulation dimension ($d = 3$, unless we quantify diffusivity in a given direction), N_H is the total number of hydrogen atoms in the simulation, and $r_i(t)$ is the position of atom i at time t . As a result, D is a measure of hydrogen diffusivity in the simulation of the square of average N_H atoms displacement.

We consider diffusion as a random transition between local stable states in order to model the effect of temperature on hydrogen diffusion in alloys [19,31,32]. The hydrogen atom transition activation energy based on the first-principles calculations is combined with the kMC method to quantitatively simulate the hydrogen diffusion process.

3. Results and discussion

In order to describe the spatial distribution of potential barriers, we herein develops the idea of potential well domain, which is the smallest unit that will trap hydrogen atoms effectively even at room temperature. The hydrogen transition barrier is very low inside the domain, but the barriers between potential well domains will be much higher.

In the following, hydrogen diffusion in VCr alloy structure will be discussed in three aspects. Firstly, we determine the stable alloy structures with various components and find that the stable configurations are all of higher symmetry. Therefore, we focus on the configurations with high symmetry, obtaining the hydrogen transition barrier to model the hydrogen diffusion process at various temperatures. Secondly, we examine two structures that have a diffusion difference of an order of magnitude at the same concentration and propose a one-dimensional unbalanced random walk model by studying potential energy surface, to explain why the shallow potential well can effectively slow down hydrogen diffusion. Finally, we compare the results of low concentration doping in the pure phase and demonstrate that Cr and V have different behavior, resulting in the slowest diffusion structure not in the alloy ratio of 1:1, but in the Cr content of 0.625.

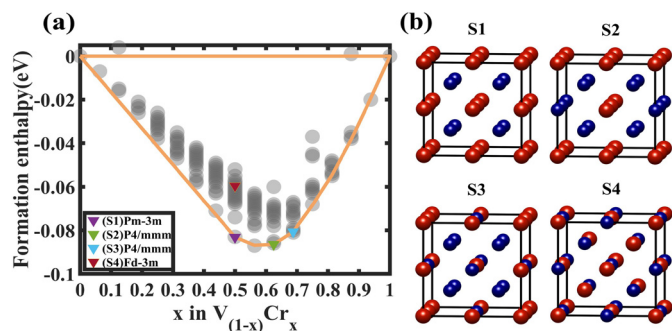


Fig. 1. (a) The formation enthalpy of VCr alloy varies with Cr concentration. (b) Four stable structures with high symmetry, namely, S1-S4 structure, where V and Cr atoms are represented by the red and blue spheres, respectively.

3.1. Stable alloy structure and hydrogen diffusion

To study hydrogen diffusion of VCr alloy, we have first determined stable structures of VCr alloy with various compositions. For the given lattice with different shapes and volumes, we can use the SAGAR program to generate the possible nonequivalent structures. Based on the total energy of the system from the first-principles calculations, the stable ground state structures are determined by the formation enthalpy, which is defined as:

$$E_f = E(V_{1-x}Cr_x) - xE(Cr) - (1-x)E(V), \quad (2)$$

where x is the ratio of Cr, also, $E(Cr)$ and $E(V)$ are the formation enthalpy in pure Cr and pure V. A probable stable structure of the alloy is the convex point of formation enthalpy curve. The formation enthalpy of most VCr binary alloy structures is negative, as illustrated in Fig. 1(a), indicating that vanadium and chromium can easily form alloys in any combination. Thus, we focus on hydrogen diffusion in VCr alloys of various proportions and investigate the variation of hydrogen diffusion coefficient as a function of Cr concentration.

As illustrated in Fig. 1(b), stable convex structures are highly symmetric, which are selected for the study of hydrogen diffusion behavior. Hydrogen is frequently distributed in the alloy's interstitial position. The center of tetrahedron is the preferred position in bcc metals because its radius is roughly twice that of octahedron, facilitating the accommodation of hydrogen atoms at low temperatures. Furthermore, it has been reported that the octahedral interstitial position is not a stable or transitory condition, but rather a saddle point [33].

We use the tetrahedral subdivision approach to find the interstitial position for the hydrogen diffusion [25]. Because S1, S2, and S3 are highly symmetrical, there are few unequal positions, namely 1, 8, and 4 unequal hydrogen sites, respectively. Hydrogen diffusion transitions only occur in the nearest neighbor, and there are 4, 25, and 15 unequal transitions, respectively. With the associated transition barriers from the first-principles calculations, we have used the kMC approach to simulate hydrogen diffusion in the alloy, as shown in Fig. 2(a). In addition, the typical transition state paths and barriers in S2 and S3 structures are shown in the supplementary materials.

At the same temperature, hydrogen diffusion in different alloy components is calculated to be slower than in pure phase, especially, the $V_{0.375}Cr_{0.625}$, has the slowest diffusion coefficient. To investigate the anisotropic effect of atomic distribution, we compare the structures with the same concentration of Cr and V, as shown in Fig. 2(b), (c). Besides S1, we have chosen another V_8Cr_8 structure S4 with strong symmetry, whose formation enthalpy is 0.024 eV larger than the ground state structure S1. Similar to S1, there is just one nonequivalent position of hydrogen in S4, and

the lowest barrier value in S4 is 0.03 eV higher than that in S1. Note that the diffusion coefficient in S4 is nearly an order of magnitude higher than S1. This demonstrates that the hydrogen diffusion is dominated by the spatial distribution of the hydrogen diffusion barrier in the alloy, rather than the height of the barrier.

3.2. Diffusion mechanism of hydrogen in VCr alloy

As shown in Fig. 2(a), for S1 and S4 with the same concentration, hydrogen diffusion in VCr alloy can vary by nearly one order of magnitude. It can be shown that the nonequivalent distribution of Cr atoms can have a substantial impact on hydrogen diffusion rate at the same component concentration. The structures of the two V_8Cr_8 alloys are very symmetric and stable, as illustrated in Fig. 1 (b) S1 and S4, and the unequal numbers of metal atoms and hydrogen atoms are also the same. Note that the distribution of potential well domain is different in S1 and S4 based on the potential energy surface study.

As shown in Fig. 3(a), structure S1's potential well domain is a plane regular quadrilateral. The initial potential energy surface shows that the minimal transition barrier in the potential well domain is 0.08 eV, which corresponds to the T-T transition path with the highest probability. The minimal transition barrier across potential well domain is 0.26 eV, as shown by the second potential energy surface, which is another T-T transition path at the hydrogen site. The structure S1 is the most symmetrical and there are only two nonequivalent diffusion paths in the potential energy surfaces as illustrated in Fig. 3(a). In contrast, hydrogen tends to travel back and forth in the 0.08 eV potential well domain, resulting in the decrease of hydrogen diffusion coefficient.

For comparison, the structure S4 whose potential well domain is a plane regular hexagon is shown in Fig. 3(c), where the four potential well domains are in the alternate arrangement. The transition path between two potential well domain is the smallest unit, displaying on each potential energy surface. The lowest transition barrier in the potential well domain is 0.11 eV, while the minimum transition barrier between neighboring potential well domain is 0.21 eV, both of which are T-T transition pathways, as shown by the potential energy surface. Therefore, the transition between the neighboring potential well domains is remarkably difficult compared with that between the inner of potential well domain.

Compared with S4, the barrier difference between the internal potential well domain and neighboring potential well domains is found to be higher in S1 structure, making the hydrogen atoms easier to become stuck in the potential well domain in S1 structure. Thus, the hydrogen transport in S1 is slower than that in S4. As shown in Fig. 3(b), (d), the numerical simulations demonstrate the details of hydrogen diffusion in S1 and S4. Assume that hydrogen atoms begin to transit from one potential well domain to the neighboring, where the probability represents the hydrogen atom still stays in the initial potential well domain after the number of steps on the horizontal axis of the transition. The expectation trial step that one hydrogen atom need to transit to the nearest potential well domain is 10^4 in S1 structure at 300 K as illustrated in Fig. 3(b). Note that about half of hydrogen atoms are still restricted to the initial potential well domain when the transition is 10^3 steps. In contrast, the structure's S4 potential well domain is less restrictive to hydrogen. At the same temperature, all hydrogen atoms in S4 structure have completed a 10^3 step transit to another potential well domain, as illustrated in Fig. 3(d). The restrictive ability of the potential well domain reduces as temperature rises, resulting in the quicker diffusion. As corresponding to Fig. 2(a), the diffusion coefficient of S1 is calculated to be much lower than that of S4, due to the larger barrier between the neighboring potential

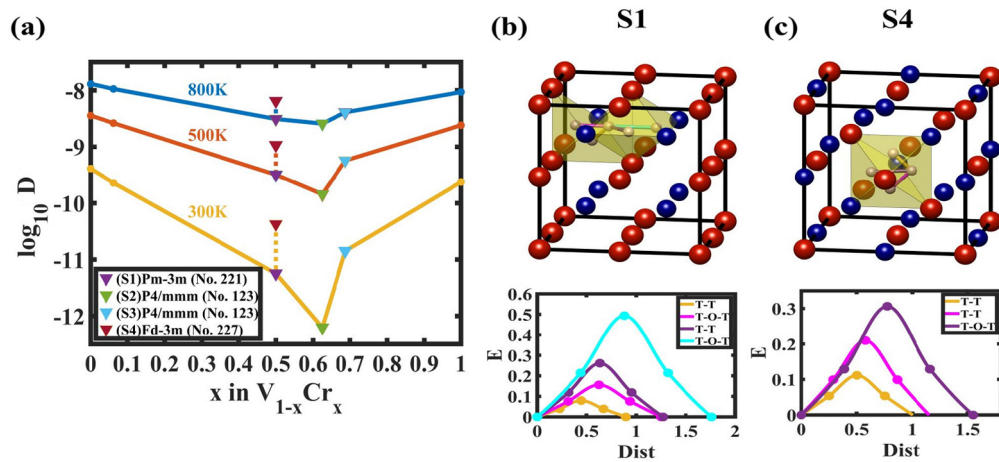


Fig. 2. (a) The diffusion curves of various alloy structures which is employed by KMC method at various temperatures. (b), (c) Comparison of all nonequivalent potential wells in V_8Cr_8 structures S1 and S4, where T and O denote tetrahedral and octahedral interstitial sites, respectively.

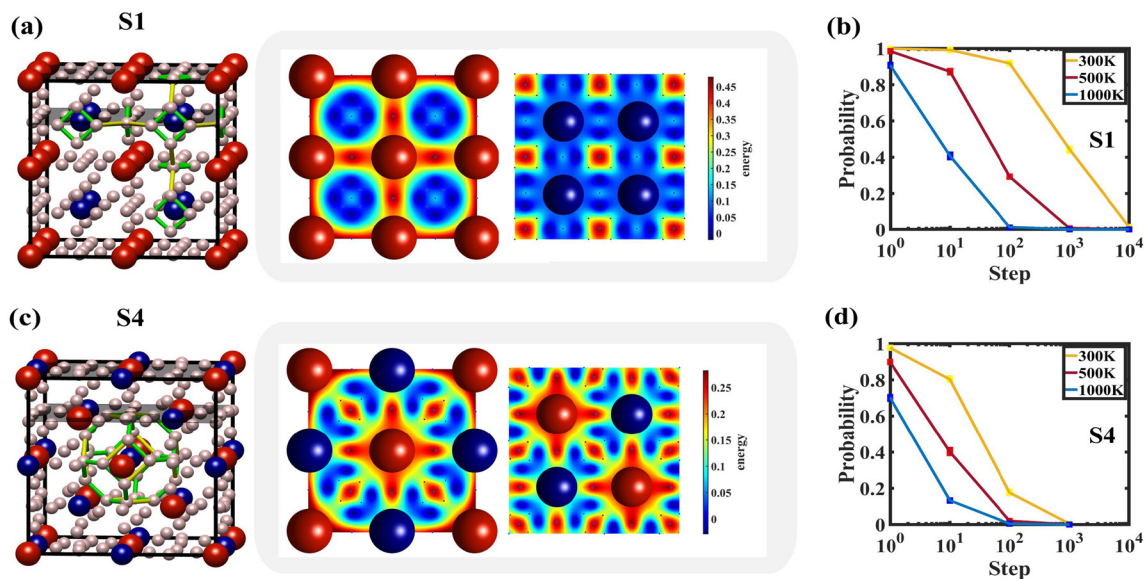


Fig. 3. (a), (c) Potential well domain and potential energy surface of structures S1 and S4, where the grayish spheres represent the all possible occupied sites in the process of hydrogen atom hopping, and where the yellow and green bonds represent the hopping across and in the potential well domain, respectively. (b), (d) Numerical simulation is used to examine the probable well domain transition of structures S1 and S4.

well domains. Previous studies indicated that the diffusion coefficient was primarily determined by the diffusion prefactor (D_0) and the transition activation energy, in which a high potential barrier will be required to limit hydrogen atom diffusion. It is found that the VCr alloy structure with shallow potential well domain, can make hydrogen migration outwards difficult and also lead to slow hydrogen diffusion.

Due to the complex atomic distribution in alloys, hydrogen diffusion usually involves transitions with different height barriers. To uncover the mechanism of the slow hydrogen diffusion, we propose a one-dimensional random walk model for simplicity, which is shown in the supplementary materials. We take a cell containing four atoms as an example, thus the transition probability matrix is a 4×4 matrix as follows. If all the transition probability is the same as:

$$P^{Balanced} = \begin{bmatrix} 0 & 0.5 & 0 & 0.5 \\ 0.5 & 0 & 0.5 & 0 \\ 0 & 0.5 & 0 & 0.5 \\ 0.5 & 0 & 0.5 & 0 \end{bmatrix}, \quad (3)$$

this is a balanced model, otherwise, the transition probability is not all the same as:

$$P^{Unbalanced} = \begin{bmatrix} 0 & 0.5 & 0 & 0.5 \\ 0.5 & 0 & 0.5 & 0 \\ 0 & 0.2 & 0 & 0.8 \\ 0.2 & 0 & 0.8 & 0 \end{bmatrix}, \quad (4)$$

this is a unbalanced model.

To amplify the variation in probability distribution at different places, the vertical axis is $-1/\log_{10}(P)$, which is positively correlated with the probability distribution. When the probabilities of random walking on the left and right are balanced, the probability distribution is a normal distribution with only one maximum at the initial location. When the left and right probabilities are unbalanced, the maximum and minimum probabilities alternately appear near the initial point as shown in Fig. 4(a). More importantly, for the positions far from the initial point, the probability distribution is smaller than the normal distribution, therefore, the corresponding net diffusion is slower. This is due to the increased

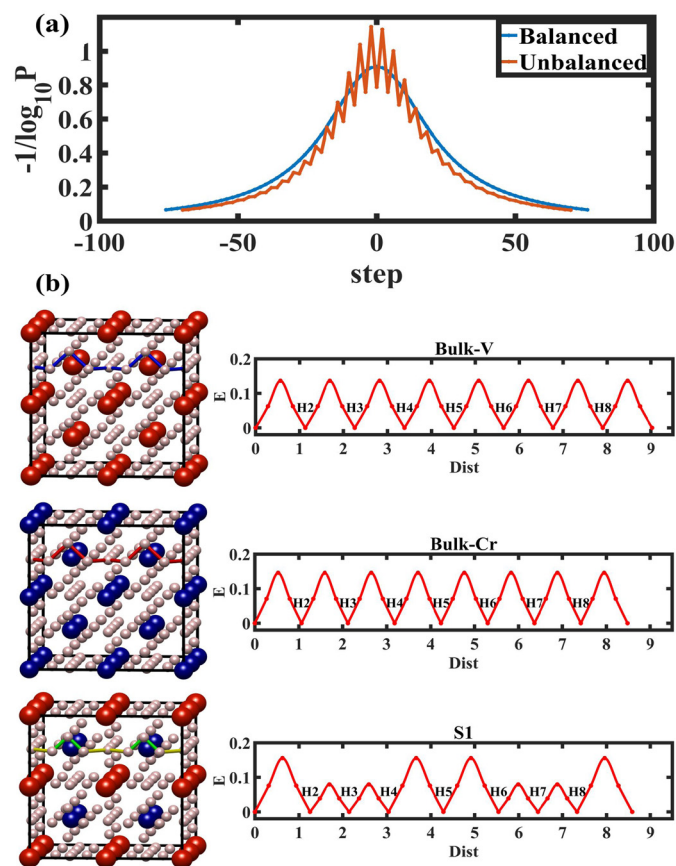


Fig. 4. (a) A one-dimensional unbalanced random walk model of pure phase and alloy hydrogen diffusion. (b) Pure phase and alloy hopping path and corresponding barriers

likelihood of hydrogen atom being stuck in NO. 3 or 4 due to the periodic boundary condition.

This phenomenon is similar to pure phase and alloy hydrogen diffusion. As illustrated in Fig. 4 (b), each hydrogen atom in the pure phase has four equivalent T-T transition pathways and two equivalent T-O-T transition paths. Because the transition barrier distribution is rather uniform and there is no potential well domain, the pure phase diffuses fast. In comparison to the pure phase, the potential barrier value of the S1 alloy structure is smaller, but a sequence of closed shallow potential well domain have formed. As a result, hydrogen atoms are trapped in the local potential well domain and they are difficult to diffuse outward, which can also slow down the overall hydrogen diffusion.

3.3. Impact of low concentration doping to the H diffusion

To further analyze the possible well domain for the hydrogen diffusion in vanadium chromium alloys, we consider the structures of pure phase doped with a small amount of elements. Taking $V_{15}Cr$ as an example, it reveals the formation of a potential well domain that can confine hydrogen atoms near a single Cr, as illustrated in Fig. 5 (a). Among them, the potential well domain's boundary potential barrier value is high, while the potential well domain's internal potential barrier value is low. The potential well domain's exterior potential barrier value gradually returns to the normal value. For the $V_{15}Cr$ structure, there is no potential well domain that can confine the hydrogen atom around a single V in the structure's center. However, V doping raises the possible barrier around V, as illustrated in Fig. 5 (b).

In both $V_{15}Cr$ and $V_{15}Cr$, the hydrogen diffusion will be slowed down similarly. However, the mechanisms of the two pure phase doped elements are completely different, especially for the potential barrier distribution. Therefore, the hydrogen diffusion behavior will become different as the doping concentration increases, and the slowest hydrogen diffusion is not found in the structure of $V_{0.5}Cr_{0.5}$.

4. Conclusion

Combining the first-principles calculations and kinetic Monte Carlo simulation, we have theoretically investigated the thermodynamic stability of VCr alloy and hydrogen atom diffusion. We identified the stable structures of various concentrations by the formation enthalpy convexhull, where the stable structures almost hold the high symmetry. Hydrogen diffusion in VCr alloy will be substantially slower than in pure phase, which is consistent with previous studies. However, it is contrary to the previous assumption that the high potential barrier will decrease diffusion. It is worth noting that the alloy contains a series of continuous closed reversible low potential well domains, which allow hydrogen atoms to be trapped in the potential well domain and slow down the net diffusion of hydrogen in the alloy. A one-dimensional unbalanced random walk model is proposed to uncover the physical origin of the slow hydrogen diffusion in the alloy, in which the unequal diffusion probability will efficiently decrease the diffusion coefficient. This demonstrates that the spatial distribution of the barrier, rather than its height, plays the most important role in the net diffusion. Our findings will be of great significance for understanding the migration of hydrogen atoms in VCr alloys.

CRedit authorship contribution statement

Shu-Ming Wu: Writing – original draft, Visualization, Validation, Methodology, Investigation, Formal analysis, Data curation, Conceptualization. **Chang-Chun He:** Writing – review & editing, Visualization, Software, Formal analysis. **Yu-Jun Zhao:** Writing – review & editing. **Rong Liu:** Writing – review & editing. **Xiao-Bao Yang:** Writing – review & editing, Supervision, Resources, Project administration.

Declaration of competing interest

The authors declare that they have no known competing financial interests or personal relationships that could have appeared to influence the work reported in this paper.

Data availability

The data that has been used is confidential.

Acknowledgement

This work was supported by Guangdong Basic and Applied Basic Research Foundation (Grant No. 2021A1515010328, 202201010090), and the National Natural Science Foundation of China (Grant No. 12074126).

Appendix A. Supplementary material

Supplementary material related to this article can be found online at <https://doi.org/10.1016/j.physleta.2023.128701>.

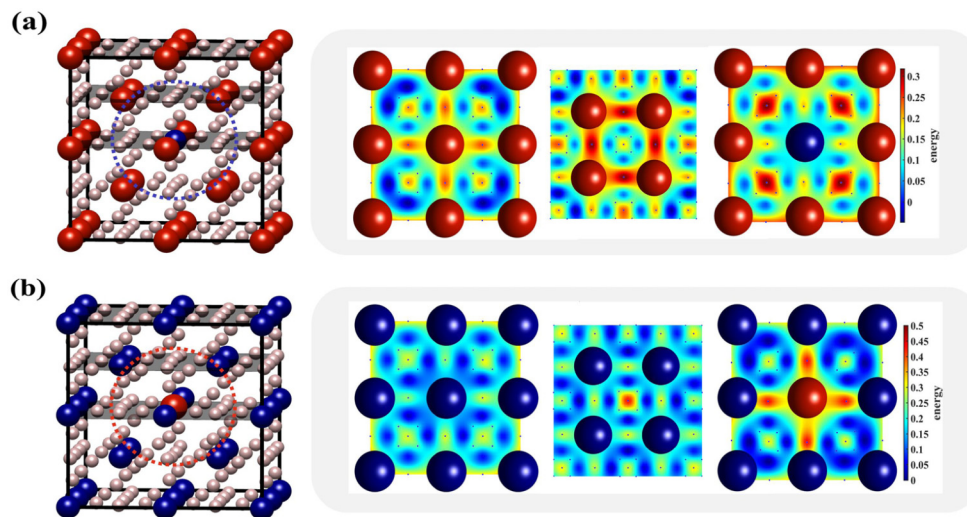


Fig. 5. (a), (b) Display of the crystal structure and potential energy surface of $V_{15}Cr$ and VCr_{15} . V and Cr atoms are represented by the red and blue spheres, respectively. Also, the possible sites for hydrogen hopping are represented by the black spots in the energy landscape profile.

References

- [1] M. Dadfarnia, P. Novak, D.C. Ahn, J.B. Liu, P. Sofronis, D.D. Johnson, I.M. Robertson, Recent advances in the study of structural materials compatibility with hydrogen, *Adv. Mater.* 22 (10) (2010) 1128–1135, <https://doi.org/10.1002/adma.200904354>.
- [2] J. Song, W.A. Curtin, Atomic mechanism and prediction of hydrogen embrittlement in iron, *Nat. Mater.* 12 (2) (2013) 145–151, <https://doi.org/10.1038/nmat3479>.
- [3] D. Hardie, E. Charles, A. Lopez, Hydrogen embrittlement of high strength pipeline steels, *Corros. Sci.* 48 (12) (2006) 4378–4385, <https://doi.org/10.1016/j.corsci.2006.02.011>.
- [4] X. Li, X. Ma, J. Zhang, E. Akiyama, Y. Wang, X. Song, Review of hydrogen embrittlement in metals: hydrogen diffusion, hydrogen characterization, hydrogen embrittlement mechanism and prevention, *Acta Metall. Sin.* 33 (6) (2020) 759–773, <https://doi.org/10.1007/s40195-020-01039-7>.
- [5] M. Dadfarnia, A. Nagao, S. Wang, M.L. Martin, B.P. Somersday, P. Sofronis, Recent advances on hydrogen embrittlement of structural materials, *Int. J. Fract.* 196 (1–2) (2015) 223–243, <https://doi.org/10.1007/s10704-015-0068-4>.
- [6] S. Bechtle, M. Kumar, B. Somersday, M. Launey, R. Ritchie, Grain-boundary engineering markedly reduces susceptibility to intergranular hydrogen embrittlement in metallic materials, *Acta Mater.* 57 (14) (2009) 4148–4157, <https://doi.org/10.1016/j.actamat.2009.05.012>.
- [7] D.N. Tafen, First-principles-based kinetic Monte Carlo studies of diffusion of hydrogen in Ni–Al and Ni–Fe binary alloys, *J. Mater. Sci.* 50 (9) (2015) 3361–3370, <https://doi.org/10.1007/s10853-015-8885-4>.
- [8] P. Kamakoti, D.S. Sholl, Ab initio lattice-gas modeling of interstitial hydrogen diffusion in CuPd alloys, *Phys. Rev. B* 71 (1) (2005) 014301, <https://doi.org/10.1103/PhysRevB.71.014301>.
- [9] D.E. Jiang, E.A. Carter, Diffusion of interstitial hydrogen into and through bcc Fe from first principles, *Phys. Rev. B* 70 (6) (2004) 064102, <https://doi.org/10.1103/PhysRevB.70.064102>.
- [10] J. Sanchez, J. Fullaer, C. Andrade, P.L. de Andres, Hydrogen in α -iron: stress and diffusion, *Phys. Rev. B* 78 (1) (2008) 014113, <https://doi.org/10.1103/PhysRevB.78.014113>.
- [11] L. Semidey-Flecha, D.S. Sholl, Combining density functional theory and cluster expansion methods to predict H₂ permeance through Pd-based binary alloy membranes, *J. Chem. Phys.* 128 (14) (2008) 144701, <https://doi.org/10.1063/1.2900558>.
- [12] B. Predel, Eu–Ge (Europium–Germanium), in: O. Madelung (Ed.), *Dy–Er – Fr–Mo*, vol. e, in: *Landolt–Börnstein – Group IV Physical Chemistry*, Springer-Verlag, Berlin/Heidelberg, 1995, pp. 1–2.
- [13] T. Matsunaga, M. Kon, K. Washio, T. Shinozawa, M. Ishikiriya, TiCrVMo alloys with high dissociation pressure for high-pressure MH tank, *Int. J. Hydrog. Energy* 34 (3) (2009) 1458–1462, <https://doi.org/10.1016/j.ijhydene.2008.11.061>.
- [14] G. Mazzolai, Some physical aspects of hydrogen behaviour in the H-storage bcc alloys Ti₃₅V₅Cr_{65-x}, Ti₄₀VMn₅₀Cr₁₀ and TiCr_{97.5}Mo_{2.5}, *Int. J. Hydrog. Energy* 33 (23) (2008) 7116–7121, <https://doi.org/10.1016/j.ijhydene.2008.07.059>.
- [15] D.J. Pine, R.M. Cottis, Diffusion and electrotransport of hydrogen and deuterium in vanadium-titanium and vanadium-chromium alloys, *Phys. Rev. B* 28 (2) (1983) 641–647, <https://doi.org/10.1103/PhysRevB.28.641>.
- [16] H. Nakajima, M. Yoshioka, M. Koiwa, Electromigration of hydrogen in vanadium and its alloys, *Acta Metall.* 35 (11) (1987) 2731–2736, [https://doi.org/10.1016/0001-6160\(87\)90272-0](https://doi.org/10.1016/0001-6160(87)90272-0).
- [17] S. Tanaka, H. Kimura, Solubility and diffusivity of hydrogen in vanadium and its alloys around room temperature, *Trans. JIM* 20 (11) (1979) 647–658, <https://doi.org/10.2320/matertrans1960.20.647>.
- [18] Y. Lu, M. Gou, R. Bai, Y. Zhang, Z. Chen, First-principles study of hydrogen behavior in vanadium-based binary alloy membranes for hydrogen separation, *Int. J. Hydrog. Energy* 42 (36) (2017) 22925–22932, <https://doi.org/10.1016/j.ijhydene.2017.07.056>.
- [19] A.J. Samin, D.A. Andersson, E.F. Holby, B.P. Uberuaga, First-principles localized cluster expansion study of the kinetics of hydrogen diffusion in homogeneous and heterogeneous Fe–Cr alloys, *Phys. Rev. B* 99 (1) (2019) 014110, <https://doi.org/10.1103/PhysRevB.99.014110>.
- [20] G. Kresse, D. Joubert, From ultrasoft pseudopotentials to the projector augmented-wave method, *Phys. Rev. B* 59 (3) (1999) 1758–1775, <https://doi.org/10.1103/PhysRevB.59.1758>.
- [21] G. Makov, M.C. Payne, Periodic boundary conditions in ab initio calculations, *Phys. Rev. B* 51 (7) (1995) 4014–4022, <https://doi.org/10.1103/PhysRevB.51.4014>.
- [22] J.P. Perdew, K. Burke, M. Ernzerhof, Generalized gradient approximation made simple, *Phys. Rev. Lett.* 77 (18) (1996) 3865–3868, <https://doi.org/10.1103/PhysRevLett.77.3865>.
- [23] J.P. Perdew, K. Burke, M. Ernzerhof, Perdew, Burke, and Ernzerhof reply:, *Phys. Rev. Lett.* 80 (4) (1998) 891, <https://doi.org/10.1103/PhysRevLett.80.891>.
- [24] G. Henkelman, B.P. Uberuaga, H. Jónsson, A climbing image nudged elastic band method for finding saddle points and minimum energy paths, *J. Chem. Phys.* 113 (22) (2000) 9901–9904, <https://doi.org/10.1063/1.1329672>.
- [25] C.-C. He, J.-H. Liao, S.-B. Qiu, Y.-J. Zhao, X.-B. Yang, Biased screening for multi-component materials with structures of alloy generation and recognition (SAGAR), *Comput. Mater. Sci.* 193 (2021) 110386, <https://doi.org/10.1016/j.commatsci.2021.110386>.
- [26] K.J. Laidler, M.C. King, Development of transition-state theory, *J. Phys. Chem.* 87 (15) (1983) 2657–2664, <https://doi.org/10.1021/j100238a002>.
- [27] J.N. Anders Nilsson, Lars G.M. Pettersson, *Chemical bonding at surfaces and interfaces*, 2011, p. 294.
- [28] Y.-H. Zhao, M.-M. Yang, D. Sun, H.-Y. Su, K. Sun, X. Ma, X. Bao, W.-X. Li, Rh-decorated Cu alloy catalyst for improved C₂ oxygenate formation from syngas, *J. Phys. Chem. C* 115 (37) (2011) 18247–18256, <https://doi.org/10.1021/jp204961g>.
- [29] F.D. Murnaghan, The compressibility of media under extreme pressures, *Proc. Natl. Acad. Sci. USA* 30 (9) (1944) 244–247.
- [30] F. Birch, Finite elastic strain of cubic crystals, *Phys. Rev.* 71 (11) (1947) 809–824, <https://doi.org/10.1103/PhysRev.71.809>.
- [31] Y.A. Du, J. Rogal, R. Drautz, Diffusion of hydrogen within idealized grains of bcc Fe: a kinetic Monte Carlo study, *Phys. Rev. B* 86 (17) (2012) 174110, <https://doi.org/10.1103/PhysRevB.86.174110>.
- [32] X.J. Hu, Z.J. Liu, Y.G. Shen, Mechanisms of amorphous-phase-dependent grain growth in two-phase nanocomposite films: a Monte Carlo analysis, *Appl. Phys. Lett.* 92 (2) (2008) 021910, <https://doi.org/10.1063/1.2834850>.
- [33] P. Bruzzoni, R. Pasianot, A DFT study of H solubility and diffusion in the Fe–Cr system, *Comput. Mater. Sci.* 154 (2018) 243–250, <https://doi.org/10.1016/j.commatsci.2018.07.066>.